Mechanical Insights into Biomaterial Wound Healing Patches and Polyvinyl Acetate Elasticity

Muhammad Iman Sufi Suliman, Nur Nabila Mohd Nazal,
Abdul Malek Abdul Wahab, Nor Fazli Adull Manan[*]
School of Mechanical Engineering, College of Engineering,
Universiti Teknologi MARA (UiTM) 40450 Shah Alam Selangor, MALAYSIA
[*]*norfazli@uitm.edu.my*

Muhammad Ilham Bin Khalit
Department of Mechanical Engineering, Bahrain Polytechnic,
KINGDOM OF BAHRAIN

ABSTRACT

This study investigates the development of biomaterial healing patches, specifically focusing on the elastomer characteristics and hyperelastic parameters of polyvinyl acetate in lab-made skin. Three sets were evaluated: plain PVAc (Set A), a mix of PVAc with Polysiloxanes (Set B), and a combination of PVAc with PVM-MA &CMC (Set C). Mechanical properties and hyperelastic behavior were assessed using ASTM D412 type-C standard and a 40 mm/min tensile test. Set A shows higher tensile stress (0.072 MPa) and higher tensile strain (1.1324) than Sets B and C. The Mooney-Rivlin and Ogden models were identified as suitable for elastomer characteristics among various hyperelastic models; specific constants for Set A were validated through these models: μ = -0.0211, α = -2.2919 for the Ogden model, C1 = -0.0036, C2 = 0.0300 for the Mooney-Rivlin model. These findings reveal similarities in mechanical characteristics between studied materials previously developed to mimic skin seen in the pattern of the hyperelastic graph, which has significant implications in developing skin-mimicking compounds for medical applications. The paper establishes potential advances in surgical practices through medicinally treated artificial skin but underscores further research into behavior when used within artificial skins in this technology sector.

Keywords: *Mooney Rivlin; Ogden; Polyvinyl Acetate; Silicone Rubber; Tensile*

ISSN 1823-5514, eISSN 2550-164X

https://doi.org/10.24191/jmeche.v21i2.26254

Received for review: 2023-10-18
Accepted for publication: 2024-02-26
Published: 2024-04-15

Introduction

The skin is a significant component of the body. It is essential in shielding the internal organs and parts of the body from external threats such as viruses, according to El-Serafi [1]. Recent years have seen a surge in interest in skin technology, and further study may assist in enhancing existing leather and skin applications, as stated in Manan's paper [2]. Unfortunately, the study findings could differ for each person depending on the state of their skin. This virus is more prone to infect skin that has been injured or otherwise compromised. As a direct result, the body and its immune system will lose several essential nutrients, according to Thirumdas et al. [3]. When it comes to most serious injuries, such as being burned, the body has difficulty producing new skin quickly if the damaged skin covers a large region. Nevertheless, the healing patch has the potential to be the answer to the problem of skin damage, and it also continues to undergo development and improvement.

Artificial skin is an alternative to natural skin if an emergency is needed because such an alternative can protect the skin from infection over an extended length of time, based on Tu's paper [4]. The behaviors and qualities of actual skin are identical to human skin characteristics. In addition, according to Nachman and Agarwal, artificial skin has the typical mechanical qualities seen in human skin, such as the ability to prevent any disease or viruses from infecting the body [5]-[6]. Temporary skin is referred to as a wound-healing patch. However, permanent replacement of skin requires a skin donor. Gottrup mentions that throughout human history, people have looked for different materials that may speed up the healing process of wounds [7]. The healing process would be affected differently depending on the primary component of the medication or treatment used.

Silicone is a polymer that includes silicon, oxygen, carbon, and hydrogen, in addition to another secondary element by Dabrowska and Levier [8]-[9]. Silicones may also contain other components. The selection of materials is to be combined with biomaterial to manufacture a skin layer in the laboratory for use as a wound patch. Silicone has a refractive index of 1.3 to 1.5, which may be modified by incorporating several compounds and structures of various human skin optical properties mentioned by Dabrowska [8].

The comprehensive exploration of hyperelastic characteristics in this study is pivotal, as it provides valuable insights into material behavior under different loads and serves as a fundamental tool for engineers in designing tailored materials, optimizing product designs, and ensuring quality control. It uses a biomaterial wound healing patch with some polyvinyl acetate. This plan will benefit the wound healing patch's tensile strength, as Nazali stated [10]. This patch will play a significant part in the medical operation lobby, where it will be utilized to conceal the wound created during the procedure. When complete, it will compile the raw data into a table and determine the amount

of stress, strain, and stretch. A hyperelastic model, such as the Ogden or Mooney-Rivlin model, will be used to analyze the data.

Methodology

Figure 1 shows the experimental approach to examining the mechanical properties of biomaterial samples. All the preparations and testing of samples use the American Society for Testing and Materials (ASTM) D412 Type C standards.

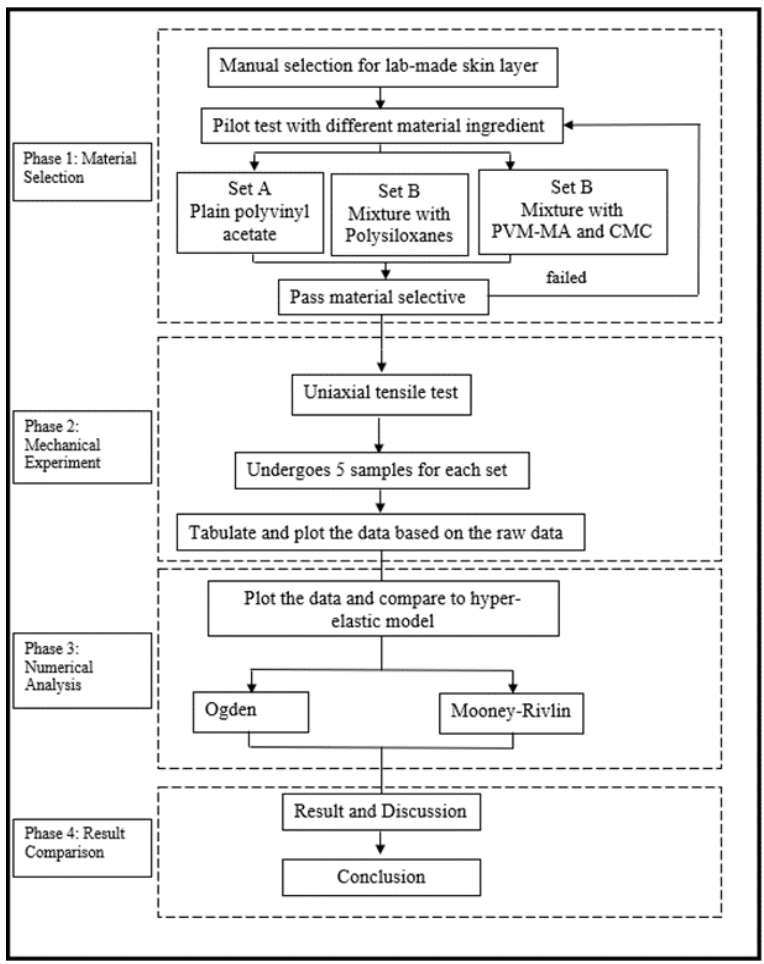

Figure 1: General methodology

Phase 1: Sample preparation

The wound healing patch samples comprise the base of the pieces from the silicone rubber, water, C27H48O20 (cornstarch), and emulsifier. According to Kasim [11], cornstarch can enhance the performance of biopolymer edible coating. The emulsifier works as a mixing agent to mix the oil-based component with the water-based component, such as silicone rubber with water, referring to the statement from Rahman [12]. The composition of the silicone rubber and other elements is specifically crafted to attain flexibility and high tensile strength. Notably, more silicone rubber is necessary to achieve superior tensile strength than other components. This formulation's weightage is informed by the findings in Nazali's and Oleiwi's papers [13]-[14]. The difference between each set was the amount of polyvinyl acetate. The well-known materials for the human skin, such as elastomers and silicone in medical applications, can be selected. For Set A, it is a plain polyvinyl acetate without any other component, while for Set B, the polyvinyl acetate mixes with the Polysiloxanes.

On the other hand, Set C is the mixture of polyvinyl acetate and Polymethyl Vinyl Ether-Malevich Anhydride (PVM-MA) Copolymer and Sodium Carboxymethylcellulose (CMC). Every composition of Sets A, B, and C has the same percentage, as shown in Table 1. The composition of the mixing agent is shown in Table 2.

Table 1: Percentage composition of the sample

	Silicone rubber (wt%)	Water (wt%)	Cornstarch (wt%)	Emulsifier (wt%)
Material composition	55	20	10	5

Table 2: Percentage composition of the mixing agent

Composition	Polyvinyl acetate (wt%)	Polysiloxanes (wt%)	PVM-MA and CMC (wt%)
Set A	10	0	0
Set B	7	3	0
Set C	7	0	3

Phase 2: Experimental tensile test procedure

The samples were prepared into dumbbell shapes based on the ASTM D412 type C, as shown in Figure 2 by Johnston [15]. The standard is for the elastomer sample that undergoes the tensile test. The SHIMADZU AG-IC 50 kN was used for the tensile test and material elongation. The speed rate of the machine was set up to 40 mm/min for each sample. The data was recorded

from zero loads until the piece reached the break and the fracture point. Figure 2 presents the uniaxial tensile test on the five samples for each set.

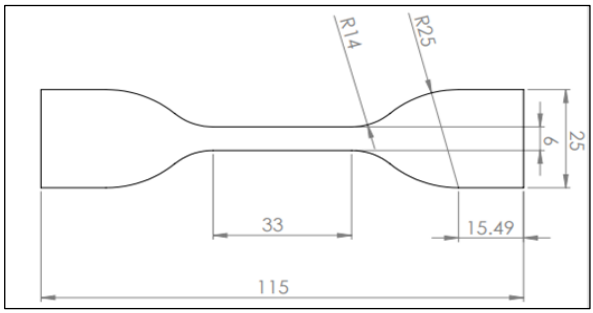

Figure 2: ASTM D412 type C, units in mm

Phase 3: Analytical development

The machine recorded the stroke and load values and manually calculated the stress, strain, and stretch. From the estimated data, the graph of load extension, stress-strain, and stress stretch was plotted by Qamar [16]. The equation (1), based on the formula obtained from He's paper on stress, describes the relationship between force and area [17]. Stress formula, which is force over the area:

$$\sigma = \frac{F}{A} \tag{1}$$

where;

σ = Stress, Pa
F = Force, N
A = Area, m^2

While for the strain and stretch, as shown in Equations (2) and (3):

$$\varepsilon = \frac{\Delta L}{L} \tag{2}$$

$$\lambda = \varepsilon + 1 \tag{3}$$

where;

ε = strain, no unit
ΔL = Different length, mm
L = Original length, mm
λ = Stretch, no unit

Then, add the data into the formula of the hyperelastic model like the Ogden model and Mooney Rivlin Model as coding. The hyperelastic model is the theoretical result to be discussed with the experimental results. By using the incompressible material formula in Equations (6) and (7), the value of the material constant of strain hardening (α) and material constant of stress (μ) in the Ogden model and for the Mooney Rivlin model, the value of the material constant, C_1 and C_2 can be calculated. The incompressible material formula is from the general formula that had been differentiated. The experimental result has been compared and discussed with the theoretical result.

In this study, we utilize the Ogden model, and its general formulation is expressed as Equation (4) [18]. This equation captures the essential characteristics of hyperelastic materials, providing a foundation for understanding their behavior under different loading conditions. Simultaneously, we refer to the general formula for the Mooney Rivlin model, denoted as Equation (5) [19]-[21], to enhance our understanding. The details of the Mooney Rivlin model are sourced from the works of Kumaraswamy, Soares, and Mao, contributing valuable insights into the non-linear mechanical properties of the materials under investigation:

$$W = \sum_{i=0}^{N} \frac{\mu}{\alpha} (\lambda_1^{\alpha_i} + \lambda_2^{\alpha_i} + \lambda_3^{\alpha_i} - 3) \tag{4}$$

$$W = C_1(\bar{I_1} - 3) + C_2(\bar{I_2} - 3) \tag{5}$$

where;

λ_j = (j=1,2,3) is the principal stretch ratio, no unit
α = Material constant related to strain hardening, no unit
μ = Material constant related with shear modulus, MPa
I1 = First invariant deviatoric component of the left Cauchy-Green deformation tensor
I2 = Second invariant deviatoric component of the left Cauchy-Green deformation tensor

The incompressible material formula for the Ogden model is Equation (6) and for the Mooney Rivlin model, as Equation (7):

$$\sigma = \frac{2\mu}{\alpha} (\lambda^{\alpha} - \lambda^{-\frac{\alpha}{2}}) \tag{6}$$

$$\sigma = 2(1 - \lambda^{-3}) * \lambda(C_1 - C_2) \tag{7}$$

where;

σ = Predicted tensile stress
C_1, C_2 = Mooney Rivlin's material constants

Those formulas were adopted based on the formulas of hyperelastic models for biomaterial. It is a concept of stress-strain energy density function.

Phase 4: Result comparison

The result was compared between the sets based on the tensile stress, strain, and Young's Modulus. The tensile stress was compared with Ni Annaidh's studies [22], whereas Young's Modulus was compared with Manickam's paper [23].

Results and Discussion

One of the essential steps is to understand the impact of the various process parameters to acquire an elastic quality comparable to that of human skin and the durability of polyvinyl acetate. Therefore, in this part, an analysis of the impacts of the various material compositions on the different process parameters was carried out.

Experimental tensile properties

Table 3 displays the strain dispersion values corresponding to each composition variation. It is essential to locate the graph that provides the best possible fit to the experimental data to acquire the mechanical characteristics of the material parameter. Table 3 shows that Set A has the highest strain value, followed by Set B and Set C. The higher strain value chooses the highest composition, with the stress at 0.072 MPa. Its elasticity would be proportional to the strain given to it: the more significant the strain, the greater the elasticity of the sample. The standard deviation for the tensile stress, strain, and Young's Modulus is measured to indicate the modest results of the dispersion value. The primary function of the error bar is to show if the testing performance aligns with the findings. The standard deviation of the tensile stress, strain, and Young's Modulus are all shown in Table 3. The value of the standard deviation for each percentage of the samples is acceptable even though the value is low.

The tensile stress, strain value, and Young's modulus were evaluated to measure the mechanical characteristics of the various sample sets. The plain polyvinyl acetate (Set A) achieved the greatest tensile stress value at 0.072 MPa. It was found that adding a second agent reduced the sample's elasticity and rendered it unfit for molding into a dog bone. It implies that simple polyvinyl acetate preserves its elasticity better than the other agents and has the highest compositional limit for mixing.

It is important to remember to put these results into perspective; according to Ni Annaidh's analysis [22], human skin can sustain tensile stress up to 21.6 MPa. Thus, plain polyvinyl acetate has a tensile strength comparable to human skin. Set A's highest strain value was 1.1324, with a standard

deviation of 0.1843. It shows that Set A is more flexible than the other sets and can withstand more deformation.

Table 3: The standard deviation of tensile stress, strain, and Young's modulus of different compositions of the sample

		Set A	Set B	Set C
a	Tensile stress (MPa)	0.072	0.065	0.031
	Standard deviation	0.1843	0.4773	0.2133
b	Strain (No unit)	1.1324	0.8840	0.5395
	Standard deviation	0.1843	0.4773	0.2133
c	Young's modulus (MPa)	0.8754	1.2389	0.7467
	Standard deviation	0.0013	0.0006	0.0021

Additionally, Table 3 illustrates that Young's Modulus value for Set B is 1.2389 MPa, surpassing values observed in the other sample sets. Notably, this value considerably exceeds the Young's Modulus range reported by Manickam for the agar phantom, which fell within the 0.052 MPa to 0.448 MPa [23]. These results underscore the significant influence of composition on the mechanical properties of the sample sets, with Set B demonstrating notably higher stiffness than the other sets.

Overall, these findings imply that altering the composition of the sample sets can modify their mechanical characteristics. Set B and plain polyvinyl acetate are attractive materials for various applications due to their high rigidity and high tensile stress. More study is necessary to fully realize these materials' potential and improve their mechanical properties for multiple applications.

Biomechanical properties (hyperelastic properties)

The stress-stretch graph is shown in Figure 3. The value of the stress was taken between 0 MPa and 0.044 MPa. The stretch value is calculated by adding 1 to the amount of strain, as shown in Equation 3.

Figure 3 compares the sample sets with Set C's fracture point of 0.031 MPa. When the stress reaches 0.0438 MPa, Set A demonstrates the highest stretch. The introduction of an additional component in Sets B and C leads to a dilution effect within the polyvinyl acetate structure, primarily attributed to the inclusion of extra water content. Consequently, the structural bonds in Sets B and C become looser, creating a distinctive characteristic compared to Set A. Set A, with a higher stretch value, may exhibit enhanced durability due to its more tightly bonded structure, rendering it less susceptible to breakage. This observation underscores the nuanced impact of additional components on the structural integrity and mechanical properties of polyvinyl acetate-based materials in each set. Moreover, the fact that Set A can endure more deformation before splitting suggests a higher elasticity than the other sets. On

the other hand, Set C may display lower ductility and increased brittleness as it reaches its fracture point at a lower stress value than the different sets.

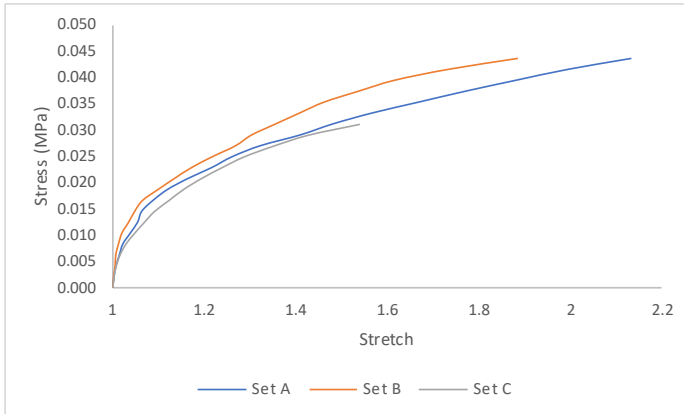

Figure 3: The graph of stress against strain for different sets of mixture

According to Jiang et al. [24], the Mooney-Rivlin and Ogden models suit the elastomer characteristic or rubber-like material. The hyperelastic model's graph produces the curve regions, such as the elastic and plastic regions. Hyperelastic models, specifically the Ogden and Mooney-Rivlin models, were conducted to evaluate the sample sets' compositional parameters. The constant values for these models are displayed in Table 4. The Mooney-Rivlin model provides the relationship between stress and strain for a hyperelastic material, whereas the Ogden model describes the strain-energy density function of a hyperelastic material.

Table 4 presents constants relating to the Ogden and Mooney-Rivlin hyperelastic models for three unique sets of materials. The Ogden model uses `μ` (mu) and `α` (alpha) to describe the initial stiffness and nonlinearity of stress-strain behavior, where typically positive constants would be expected. Negative values, as given, suggest unconventional material behavior or possible anomalies in experimental or model applications. The Mooney-Rivlin model employs `C1` and `C2`, with `C1` denoting compliance at small deformations and `C2` reflecting the response at more significant strains; positive constants are usually anticipated, suggesting resistance to deformation.

Despite the insights that Table 4 provides on the compositional characteristics of the sample sets, it is essential to acknowledge that the models used were simplified, possibly not fully capturing the materials' complex mechanical behaviors. However, the results may serve as a basis for further research and comparative analyses. Set A, being plain polyvinyl acetate

exhibits more elastic behavior according to the negative constants in both models, this demands examination due to their unconventional nature. In contrast, Set C, including PVM-MA and CMC, appears less ductile and more brittle, comparing stress-strain data and hyperelastic model predictions. The Ogden and Mooney-Rivlin models provide a preliminary understanding of the compositional parameters. However, comprehensive research is still required to fully grasp these materials' mechanical properties and optimize their performance for specific applications like wound healing patches. The negative constants throughout the table raise important considerations regarding research methodology, experimental demand, and the interpretation of data to ensure that the materials modelled adhere to realistic and practical biomedical applications.

Table 4: The characterized parameter of hyperelastic model

	Ogden		Mooney Rivlin	
	μ	α	C_1	C_2
Set A (Plain Polyvinyl Acetate)	-0.0211	-2.2919	-0.0036	0.0300
Set B (Polysiloxanes)	-0.0232	-2.3468	-0.0081	0.0391
Set C (PVM-MA and CMC)	-0.0231	-2.6932	-0.0561	0.1037

The experimental data for Set A was compared to those from the Mooney-Rivlin and Ogden models to examine the material's mechanical properties further. The comparison of the stress-stretch curve obtained from the experimental data and the hyperelastic model is shown in Figure 4. The comparison's findings demonstrate that the models can reproduce the overall pattern of the experimental data, with the hyperelastic model's stress-stretch curve having a consistent shape.

Although comparing the experimental results and the hyperelastic models provides some information on the material's mechanical characteristics, it is vital to remember that the models are simplified and might not accurately reflect the material's complicated mechanical behavior even though the comparison offers a starting point for additional investigation and can be used to enhance the material's performance for applications.

It's interesting to note that there is a similar pattern when comparing this study's findings with Nazali's research on mimicking skin growth [10]. It shows that the materials used in this study have mechanical characteristics like those of the mimic skin created in the earlier study. Particularly in the field of skin-mimicking materials for medicinal and aesthetic purposes, this resemblance may have significant consequences for possible applications of the materials.

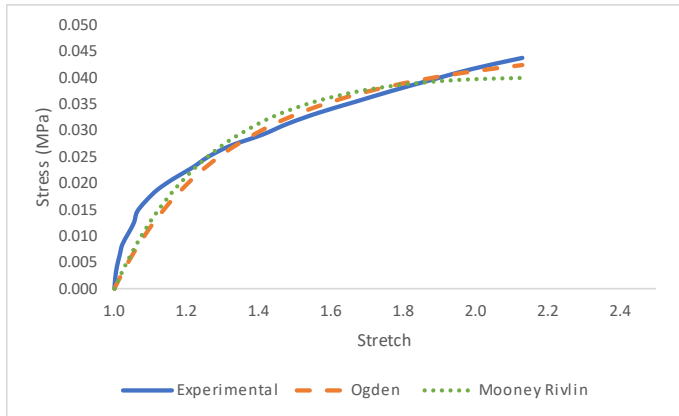

Figure 4: The comparison between the numerical and experimental graph of plain polyvinyl acetate mixture

Conclusion

The study successfully achieved its goal of quantifying the behavior of various biomaterial compositions and hyperelastic model parameters. Notably, Set A emerged as a promising biomaterial for wound healing patches, closely approximating average values for tensile stress, strain, and Young's Modulus across different weight percentages. The experimental findings highlighted that Set A exhibited the highest tensile stress (0.072 MPa) due to silicone rubber and robust structural bonding within polyvinyl acetate. Moreover, biomechanical assessments revealed that Set A demonstrated superior flexibility and durability, as evidenced by a higher stretch value of 2.13 compared to other sets. The recommendation for future research suggests exploring new mixtures compatible with the peeling test method and employing a similar numerical analysis approach. These findings contribute valuable insights to biomaterial development, emphasizing Set A's potential for effective wound healing applications.

Contributions of Authors

The authors confirm the equal contribution in each part of this work. All authors reviewed and approved the final version of this work.

Funding

This work received no specific grant from any funding agency.

Conflict of Interests

One of the authors, Abdul Malek Abdul Wahab, is a section editor of the Journal of Mechanical Engineering (JMechE). The author has no other conflict of interest to note.

Acknowledgement

Authors wish to extend our sincere gratitude to the Ministry of Higher Education, the College of Engineering at UiTM Shah Alam, and all of the members of the team for providing us with the resources and assistance that we needed in conducting this research. We incredibly grateful to everyone who helped out with this project by giving their time, expertise, and support. Your combined contributions have greatly improved the final product of this article.

References

[1] T. El-Serafi, I. T. El-Serafi, M. Elmasry, I. Steinvall, and F. Sjöberg, "Skin regeneration in three dimensions, current status, challenges and opportunities", *Differentiation*, vol. 96, pp. 26-29, 2017. doi: 10.1016/j.diff.2017.06.002

[2] N. F. A. Manan and J. Mahmud, "The effect of skin orientation on biomechanical properties," *Journal of Mechanical Engineering*, vol. 12, no. 1, pp. 67-81, 2015.

[3] R. Thirumdas, A. Kothakota, R. Pandiselvam, A. Bahrami, and F. J. Barba, "Role of food nutrients and supplementation in fighting against viral infections and boosting immunity: A review", *Trends Food Science & Technology*, vol. 110, no. 47, pp. 66-77, 2021.

[4] Y. Tu, M. Zhou, Z. Guo, Y. Li, Y. Hou, D. Wang, and L. Zhang, "Preparation and characterization of thermosensitive artificial skin with a sandwich structure", *Materials Letters*, vol. 147, pp. 4-7, 2015. doi: 10.1016/j.matlet.2015.01.163.

[5] M. Nachman and S. E. Franklin, "Artificial skin model simulating dry and moist in vivo human skin friction and deformation behaviour", *Tribology International*, vol. 97, pp. 431-439, 2016.

[6] T. Agarwal, R. Narayan, S. Maji, S. Behera, S. Kulanthaivel, T. K. Maiti, I. Banerjee, K. Pal, and S. Giri, "Gelatin/Carboxymethyl chitosan based scaffolds for dermal tissue engineering applications," *International Journal of Biological Macromolecules*, vol. 93, pp. 1499-1506, Dec. 2016. doi: 10.1016/j.ijbiomac.2016.04.028

[7] F. Gottrup, M. S. Ågren, and D. Tonny Karlsmark, "Models for use in wound healing research: A survey focusing on in vitro and in vivo adult soft tissue", *Wound Repair and Regeneration*, vol. 8, no. 2, pp. 83-89, 2000. doi: https://doi.org/10.1046/j.1524-475x.2000.00083.x

[8] A. K. Dabrowska, G. M. Rotaru, S. Derler, F. Spano, M. Camenzid, S. Annaheim, R. Stampfli, M. Schid, and R. M. Rossi, "Materials used to simulate physical properties of human skin", *Skin Research and Technology*, vol. 22, no. 1, pp. 3-14, 2016. doi: 10.1111/srt.12235

[9] R. R. Levier, M. C. Harrison, R. R. Cook, and T. H. Lane, "What Is Silicone?," *Journal of Clinical Epidemilogy*, vol. 48, pp. 513-517, 1995.

[10] N. N. M. Nazali, N. A. A. Anirad, and N. F. A. Manan, "The mechanical properties of mimic skin," *Applied Mechanics and Materials*, vol. 899, pp. 73-80, 2020. doi: 10.4028/www.scientific.net/amm.899.73

[11] R. Kasim, N. Bintoro, S. Rahayoe, and Y. Pranoto, "Optimization of the formulation of sago starch edible coatings incorporated with Nano Cellulose Fiber (CNF)," *Pertanika Journal of Science and Technology*, vol. 31, no. 1, pp. 351-372, 2022. doi: 10.47836/pjst.31.1.21

[12] S. A. Rahman, U. S. Abdullah, and S. Shaharuddin, "Formulation and antimicrobial screening of piper sarmentosum cream against staphylococcus aureus", *Pertanika Tropical Agricultural Science*, vol. 44, no. 3, pp. 527-540, 2021. doi: 10.47836/pjtas.44.3.02

[13] N. N. M. Nazali and N. F. A. Manan, "The numerical analysis of hyperelastic properties in commercial and original aloe vera gels," *Journal of Mechanical Engineering*, vol. 18, no. 3, pp. 1-20, 2021.

[14] J. K. Oleiwi, H. Mohammed, A. K. Al-Khwarizmi, S. I. Salih, J. K. Oleiwi, and H. M. Ali, "Modification of silicone rubber by added PMMA and natural nanoparticle used for maxillofacial prosthesis applications," *APRN Journal of Engineering and Applied Sciences*, vol. 14, no. 4, pp. 781-791, 2019.

[15] I. D. Johnston, D. K. McCluskey, C. K. L. Tan, and M. C. Tracey, "Mechanical characterization of bulk Sylgard 184 for microfluidics and microengineering," *Journal of Micromechanics and Microengineering*, vol. 24, no. 3, pp. 1-9, 2014. doi: 10.1088/0960-1317/24/3/035017

[16] S. Z. Qamar, M. Akhtar, T. Pervez, and M. S. M. Al-Kharusi, "Mechanical and structural behavior of a swelling elastomer under compressive loading", *Materials & Design*, vol. 45, pp. 487-496, 2013. doi: 10.1016/j.matdes.2012.09.020

[17] Q.-C. He and A. Curnier, "A more fundamental approach to damaged elastic stress-strain relations," *International Journal of Solids and Structures*, vol. 2, no. 10, pp. 1433-1457, 1995.

[18] R. W. Ogden, "Non-linear elastic deformations," *Journal of Applied Mechanics*, vo. 52, pp. 740-741, 1985.

[19] N. Kumaraswamy, H. Khatam, G. P. Reece, M. C. Fingeret, M. K. Markey, and K. Ravi-Chandar, "Mechanical response of human female breast skin under uniaxial stretching," *Journal of The Mechanical Behavior of Biomedical Materials*, vol. 74, pp. 164-175, 2017. doi: 10.1016/j.jmbbm.2017.05.027

[20] R. M. Soares and P. B. Gonc¸alves, "Large-amplitude non-linear vibrations of a Mooney-Rivlin rectangular membrane," *Journal of Sound and Vibration*, vol. 333, no. 13, pp. 2920-2935, 2014. doi: 10.1016/j.jsv.2014.02.007

[21] H. Mao, "Modeling the head for impact scenarios", in Basic Finite Element Method as Applied to Injury Biomechanics, Academic Press, Canada, 2018, pp. 469-502. doi: 10.1016/B978-0-12-809831-8.00012-X

[22] A. Ní Annaidh, K. Bruyère, M. Destrade, M. D. Gilchrist, and M. Otténio, "Characterization of the anisotropic mechanical properties of excised human skin," *Journal of The Mechanical Behavior of Biomedical Materials*, vol. 5, no. 1, pp. 139-148, 2012.

[23] K. Manickam, R. R. Machireddy, and S. Seshadri, "Characterization of biomechanical properties of agar-based tissue mimicking phantoms for ultrasound stiffness imaging techniques," *Journal of The Mechanical Behavior of Biomedical Materials*, vol. 35, pp. 132–143, 2014. doi: 10.1016/j.jmbbm.2014.03.017

[24] M. Jiang, J. Dai, G. Dong, and Z. Wang, "A comparative study of invariant-based hyperelastic models for silicone elastomers under biaxial deformation with the virtual fields method," *Journal of The Mechanical Behavior of Biomedical Materials*, vol. 136, p. 105522, 2022. doi: 10.1016/j.jmbbm.2022.105522